Int. J. Electrochem. Sci., 14 **(2019)** 1794 – 1808, doi: 10.20964/2019.02.33

International Journal of
ELECTROCHEMICAL
SCIENCE
www.electrochemsci.org

A Novel Photoelectrochemical Sensor Based on Gr-SiNWs-Si/Pt Electrode for Sensing of Hydroquinone

Hua Zhang[1,*], *Huaixiang Li*[2], *Jiao Li*[1], *Haibin Sun*[1], *Lixia Zhou*[1], *Ruihua Wang*[3]

[1] School of Materials Science and Engineering, Shandong University of Technology, Zibo 255000, P.R. China
[2] College of Chemistry, Chemical Engineering and Materials Science, Shandong Normal University, Jinan 250014, P. R. China
[3] Library, Shandong Normal University, Jinan 250014, P. R. China
[*]E-mail: zhanghua01979@sdut.edu.cn

Received: 24 October 2018 / *Accepted:* 11 December 2018 / *Published:* 5 January 2019

Herein, a graphene (Gr) and silicon nanowires (SiNWs) decorated n-silicon/platinum (Si/Pt) sensor was put forward to detect hydroquinone (HQ) in a photoelectrochemical (PEC) way. Platinum film was coated on the polished side of the n-silicon wafer by vacuum evaporation and SiNWs were fabricated uniformly on the other side of the wafer by electrochemical etching in a solution mixed by HF and ethanol with volume ratio 1:1 under illumination of scattered laser. The morphology and component of the SiNWs was characterized by SEM and EDS, respectively. The photoelectric properties of the SiNWs-Si/Pt were studied by semi-log current-voltage (log *I–V*) and photoresponse measurements. Results show that the SiNWs on the Si wafer enhance the photoelectric conversion efficiency of the Si/Pt Schottky junction by about 33% relative to Si/Pt without SiNWs. Then, graphene was prepared with Hummer method and was used to decorated the SiNWs-Si/Pt wafer to build a Gr-SiNWs-Si/Pt PEC sensor. The new sensor was used to detect HQ in a two-electrode PEC way at zero bias voltage in a linear range of 10-300 μM with a detection limit of 0.3 μM (S/N=3). Excellent selectivity of the sensor to HQ in the present of catechol (CC) and other interferences was proved by anti-interference experiment.

Keywords: Photoelectrochemical; Graphene; PEC sensor; Hydroquinone; Zero bias detection

1. INTRODUCTION

Hydroquinone (HQ), as one of phenol compound pollutants, is toxic for many organisms in the environment even at very low concentration [1]. It has long been recognized that the absorption of HQ may cause some disease like renal tube degeneration and liver function decrease [2]. However, HQ is still in mass production as a chemical raw material for the huge demand in industrial production, such

as lithography, dyes, plastics, pharmaceuticals and pesticides [3]. Thus, monitoring overdosed HQ in environment water has become a urgent task in recent years. Conventional detection methods, such as high performance liquid chromatography (HPLC) [4, 5] and gas chromatography [6], have shortages of cost expensive and time consuming. UV-vis spectrophotometry method needs a complex pretreatment for conversion of HQ to *p*-benzoquinone [7] and the results may be affected by pH, temperature and other interferences absorbing in UV spectrum. In comparison, electrochemical methods have the advantage of high efficiency, low cost and ease of use. Many literatures have been reported in the development of sensitive electrodes [8-11]. Based on electrochemical analysis, photoelectrochemical (PEC) analysis has been developed for the advantages of low background signal, rapid measurement speed, high sensitivity and ease of miniaturization in detection devices [12-15]. It is especially charming and interesting to develop PEC sensors independent of electric power supply. Unlike traditional three-electrode system, PEC sensors are mainly two-electrode systems consisting of a work electrode and a counter electrode. Reference electrode is not necessary in most PEC sensors, which permits the convenience of miniaturization and also avoids contaminants and other inconvenience from the reference electrodes.

To build a PEC sensor, it is essential to select a suitable PEC material to provide energy translated from light. Although newly developed semiconductor nanomaterials, such as nano-TiO_2 [16], nano-WO_3 [17], etc, are very popular in recent years, they suffer from instability and immaturity in laboratory stage. In comparison, production of silicon wafers has been industrialized for several decades and various types of silicon wafers have already been commercialized and ease of obtain by purchase with inexpensive price. Therefore, silicon based PEC sensors still have great potential in research works and in applications. In recent years, we have developed several PEC sensors based on silicon substrate by appropriate modification, such as by transition elements ferricyanide and oxyhydroxide [18-22].

In previous work, we reported a copper hexacyanoferrate film modified silicon electrode which has been used in HQ determination by photocurrent measurements [21]. However, the reported sensor suffers from poor linear response to HQ and great interference from catechol (CC). Therefore, it would be beneficial to develop a more sensitive PEC sensor with excellent anti-interference to CC in detection of HQ. Herein, we report a new PEC sensor based on platinum film coated phosphorus doped silicon (n-Si) wafer with new modification for selective detection of HQ in the presence of CC. In this work, graphene (Gr) was prepared by Hummer method and was used to decorate the sensor to improve the affinity of HQ on electrode. In addition, for the first time, silicon nanowires (SiNWs) were fabricated on the silicon wafer to facilitate the charge exchange between silicon wafer and the modified graphene layer. With the decoration of SiNWs and graphene, the proposed PEC sensor can be used to selectively detect HQ without being interfered by CC with a better sensitivity and a wider linear range.

2. EXPERIMENTAL

2.1 Materials and reagents

Single side polished phosphorus doped (111)-oriented silicon wafers (n-Si) with resistance of 3-5 Ω cm were purchased from Semiconductor Materials Plant, Shanghai Nonferrous Metal Institute. High purity platinum (Pt) wire (>99.99%) were purchased from Shanghai Chemical Reagent Station.

Spectroscopic purity graphite powders and graphite plates were obtained from Shanghai Chemicals, China. Ethanol, hydrogen fluride (HF wt 40 %), N, N-dimethylamide (DMF), hydroquinone (HQ), catechol (CC), KCl, Na_2HPO_4 and NaH_2PO_4 were purchased from Aladdin Industrial Corporation Company. All the chemicals were of analytical grade and were used without further purification. All solutions were prepared with double-distill water obtained from a Milli-Q water purifying system (>18 MΩ cm at 293 K). Phosphate buffer solution (PBS, pH=7.0) used in the experiment consists of 0.1 M Na_2HPO_4, 0.1 M NaH_2PO_4 and 0.2 M KCl. A DM220 high vacuum system (Shanghai Optical Electron Company, China) was used to evaporate Pt film on the polished side of n-Si wafers. Electrochemical preparation and measurements were carried out on a LK2005 electrochemical workstation (Lanlike Company, Tianjin, China).

2.2 Preparation and characterization of the photoelectrochemical (PEC) sensor

The silicon wafer (300 μm in thickness) was cleaned with hydrogen fluoride (HF 40% wt) solution and then rinsed in deionised water in ultrasonic bath for 20 min before use. About 40 nm Pt layer was deposited on the polished side of the Si wafers in a high vacuum evaporating system (5×10^{-4} Pa) and then annealed in argon atmosphere at 773 K for 20 min before naturally cooling to room temperature. Next, silicon nanowires (SiNWs) were fabricated on the unpolished side of the wafer by electrochemical etching in a mixture solution of HF (40% wt) and ethanol with volume ratio 1:1. Specifically, a 5 mW 650 nm LED laser with optical gratings was used in illumination as shown in Scheme 1.

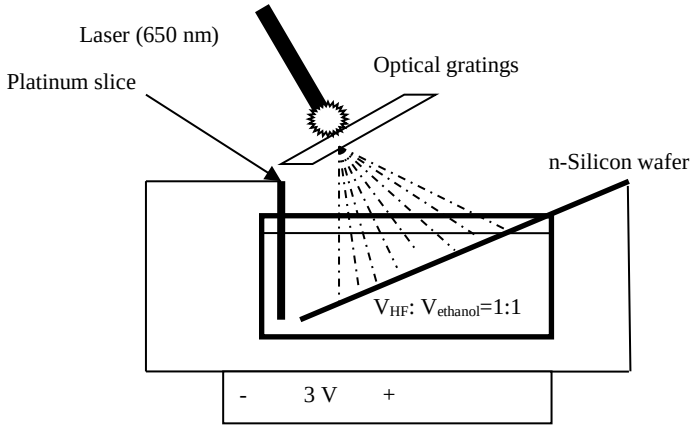

Scheme 1. Fabrication of SiNWs on n-Si wafer assisted with laser

The laser was scattered by the optical gratings to be large quantity of light spots illuminating on the silicon wafer. The wafer was jointed to the positive pole of a 3 V direct current power and a platinum slice was used as the negative pole. The etching time is 30 seconds. After etching, the wafer was observed using a FEI Sirion 200 SEM and the surface components were studied with an energy dispersive X-ray spectrometer (EDS) coupled to the SEM. The wafer was referred to as SiNWs-Si/Pt in this stage. Semi-

log current-voltage (log *I–V*) and photoresponse characteristics of the SiNWs-Si/Pt were studied by a LK2005 workstation. Finally, graphene (Gr) dispersion (5.0 $mg \cdot mL^{-1}$ in N, N-dimethylamide, DMF) was dipped on the Si side and dried in N_2 at 333K for 90 min. Preparation of graphene with Hummer method from graphite powder was described in our previous work [22]. The prepared electrode was referred to as Gr-SiNWs-Si/Pt herein. The symbol "/" means phase interface while "-" means discontinuous decoration or local area adsorption. The morphology of graphene modified wafer was observed using a Quanta 250FEG SEM and the surface components were analyzed with the coupled EDS device. In addition, FTIR was employed to study function groups of the deposited graphene on the Gr-SiNWs-Si/Pt electrode with a Nicolet 5700 FTIR spectrum.

2.3. Characteristics of the PEC sensor in detection of HQ

The PEC sensor consists of a Gr-SiNWs-Si/Pt electrode and a graphite plate electrode was used to detect HQ in pH=7 PBS solution in a two-electrode system at zero bias voltage with illumination by a 5 W white LED light. Photocurrent responses on the Gr-SiNWs-Si/Pt electrode to successive addition of 10 μM, 10 μM, 20 μM, 20 μM, 40 μM, 40 μM, 80 μM and 80 μM HQ were recorded to obtain the photocurrent curves. In comparison, Si/Pt, Gr-Si/Pt and SiNWs-Si/Pt electrode were also tested in the same conditions. The anti-interference property of the Gr-SiNWs-Si/Pt electrode was evaluated against common pollutants such as catechol (CC), Cu^{2+}, Pd^{2+}, *L*-cysteine, glutamic acid and uric acid in PEC way detection of HQ.

3. RESULTS AND DISCUSSION

3.1 SEM and EDS characterization of the SiNWs-Si/Pt

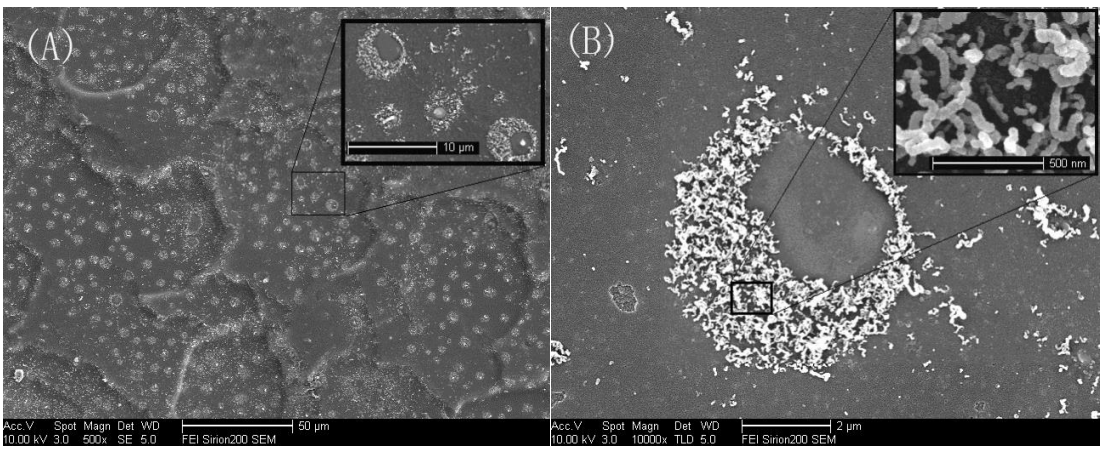

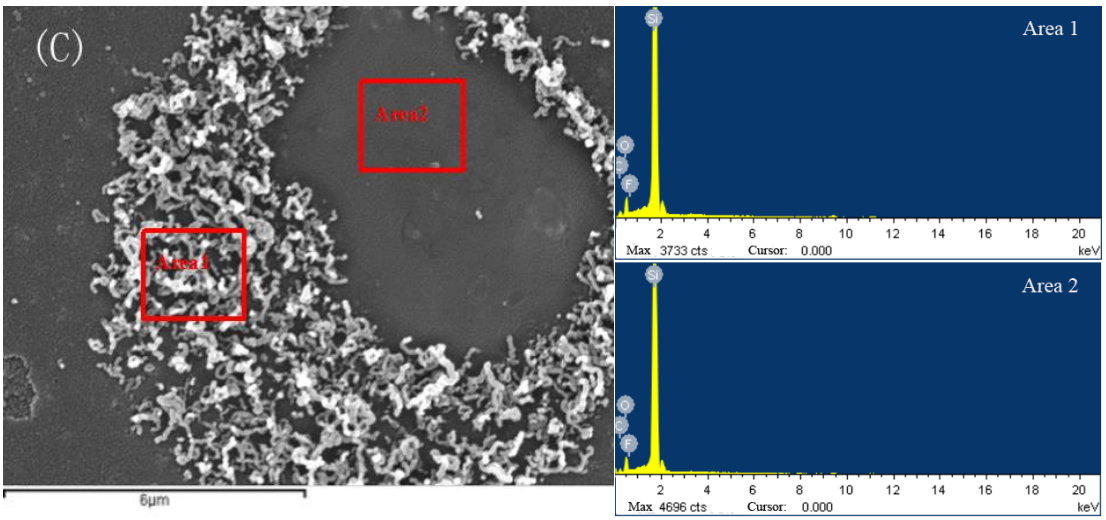

Figure 1. SEM images (A), (B) and EDS spectrum (C) of the SiNWs-Si/Pt

Fig. 1 shows the SEM morphology and the EDS results of the SiNWs-Si/Pt. Fig. 1A shows plenty of etched spots distributed uniformly on the wafer and Fig. 1B shows the morphology of the etched spots in higher magnification. The insets show the regional amplification in local area marked with black rectangles. The distribution and the shape of the etched spots are in accordance with the light spots of the laser illumination as Scheme 1 shows. Nanowires in diameter of about 50 nm and in length of less than 1 μm can be distinguished in the inset of Fig 1B. This special morphology may be ascribed to the concentrated laser induced carriers and the thermal stress in local areas caused by the laser illumination. Detail explanations are as follows:

Holes are essential in the etching process of silicon in HF solution, but holes are minority carriers in n-type silicon (n-Si). Thus light is necessary to provide electron-hole pairs in the etching process. With spotted laser illumination, etching takes place only in the illuminated areas on the n-Si wafer as Fig. 1A shows. Coupled with thermal stress which may cause crystal detachment in the laser illuminated areas, silicon etches very fast and resulted in the special morphology as shown in Fig 1A and Fig. 1B.

In order to study the components of the nanowires, energy dispersive X-ray spectrometer (EDS) analysis was employed and the results show in Fig. 1C. The analyzed areas are selected in two distinctly different areas in morphology, i.e., “Area 1” with abundant nanowires and “Area 2” without nanowires as marked in the electronic image in Fig. 1C. Results show little difference in component between the two areas as depicted in the EDS spectrum in Fig 1C. In both selected areas, Si is the predominant element with scarce O, F and C elements. The small quantity of oxygen element may owe to slight sample oxidation in the air. Trace amounts of fluorine and carbon element may come from the HF electrolyte and CO_2 in atmosphere respectively. According to the EDS results, the nanowires are mainly composed of Si element with trace impurities, therefore, are written as SiNWs herein.

3.2 Photovoltaic conversion characteristics of the SiNWs-Si/Pt electrode

Fig. 2A shows the semi-log current-voltage (log *I–V*) graphics measurements of the SiNWs-Si/Pt

(curve a, b) and the Si/Pt (curve c, d). The log *I–V* curves were measured between -0.5 V and 2.0 V bias voltages at room temperature. It can be seen, a discrimination of in dark and in light from the log *I–V* characteristics is obvious in both SiNWs-Si/Pt and Si/Pt curves. When exposed to light, electron−hole pairs generate in silicon wafers. They may recombine inside the wafer or can be introduced to the surface of the electrodes to reaction with analytes in solution to produce current signals which can be used to characterize the concentration of the analytes. In most cases, the currents are too weak to be detected for the poor electron-hole separation efficiency. However, with a Pt film coating on the n-Si, there is a static electric field build between the Pt film and the n-Si wafer, owing to the different electronic work functions of n-Si and Pt. Therefore, the photon-generated electrons and holes are separated by the electric field to the Si and the Pt side, respectively, and thus measureable current signals can be obtained. Both SiNWs-Si/Pt and Si/Pt exhibited rectifying properties with weak voltage dependence of the forward bias current and an exponential increase of the reverse bias current as shown in Fig. 2A, which are the characteristic properties of the rectifying interface [23].

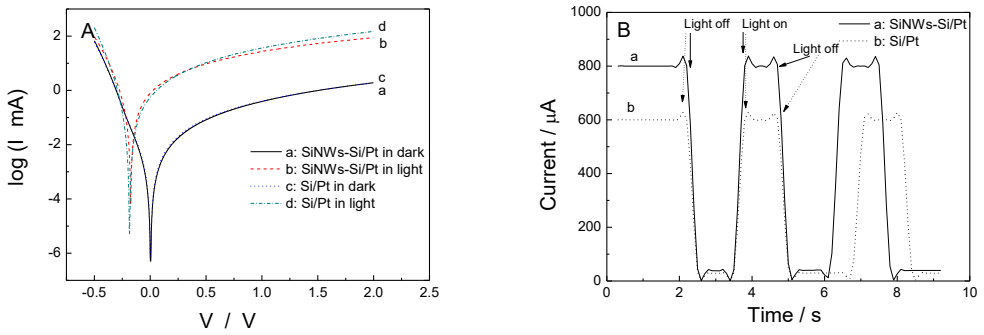

Figure 2. (A) Semi-log current-voltage (log *I–V*) characteristics of the SiNWs-Si/Pt and Si/Pt in dark and in light; (B) The transient photocurrent plots of SiNWs-Si/Pt and Si/Pt in a 5 W white light LED illumination

In order to further study the effect of the SiNWs growth on the photoresponse of the Si/Pt electrode, transient photocurrents were measured as shown in Fig. 2B. It is clear that both Si/Pt and SiNWs-Si/Pt are sensitive to the light. The photocurrent of both the Si/Pt and the SiNWs-Si/Pt increases sharply after illumination and remains almost constant until the illumination being turned off. Moreover, with the growth of SiNWs, the photocurrent increased from 600 μA on the Si/Pt electrode to 800 μA on the SiNWs-Si/Pt electrode under same experiment conditions. The SiNWs on the Si wafer seem to act as electron transmitting tunnels between the wafer and the outer circuit that enhances the obtained photocurrents. This property may be beneficial to electrochemical reactions in the double layer between electrode and solution.

3.3 SEM, EDS and FTIR characterization of the Gr-SiNWs-Si/Pt

The surface morphology of Gr-SiNWs-Si/Pt electrode was observed by a Quanta 250FEG SEM (Fig. 3A and Fig. 3B) and the surface components were studied by the coupled EDS device (Fig. 3C).

Furthermore, FTIR was employed to study the function groups in the modified graphene. It can be seen from Fig. 3A that the electrode surface was covered by flake shaped graphene with little amount of spheral aggregation. Fig. 3B is the higher magnification morphology of the center area in Fig. 3A, showing a huge specific surface area of the flake shaped graphene. It is reasonable to speculate that the modified graphene may improve the adsorption capacity of the electrode to HQ. The EDS results shown in Fig. 3C demonstrated the surface components of the Gr-SiNWs-Si/Pt electrode. The C peaks are corresponded to the main component of graphene and the O peaks come from the organic functional groups such as "-COOH" and "-OH" that often exist in Hummer method prepared graphene. The Si peaks owe to the silicon wafer substrate and the Cr element was introduced by the metal spraying pretreatment before SEM observing. Trace level of other elements may be contaminants in the experiment. The EDS spectrum in the selected area 1 shows a very strong C peak, which is in accordance with the spheral aggregation graphene in this region as depicted in the electric image in Fig. 3C. In comparison, no C signal has been detected in selected area 4 spectrum because of the cavity morphology in selected area 4. In all the EDS results, the strong Si peaks originated from the silicon substrate demonstrate a good electron transmittance property of the graphene layer, which is to the benefit of charge exchange for electrodes. Fig. 3D depicts the FTIR spectrum of the modified graphene on the electrode. The strong wide band centered at about 3300 cm^{-1} in the FTIR spectrum is corresponded to the stretching vibration of the associated O-H bond (ν_{O-H}) in carboxyl group (-COOH). The flexural vibration of O-H bond (δ_{O-H}) and the stretching vibration of C=O bond ($\nu_{C=O}$) in the carboxyl group peaks appear at about 1410 cm^{-1} and 1735 cm^{-1} in the spectrum, respectively. The peaks at about 1075 cm^{-1} are ascribed to the flexural vibration of C-H bond (δ_{C-H}) on the benzene ring framework of graphene. It can be expected that the modification of graphene with electroactive carboxyl groups may facilitate interchanges of reactants in electrochemical reactions on the electrode.

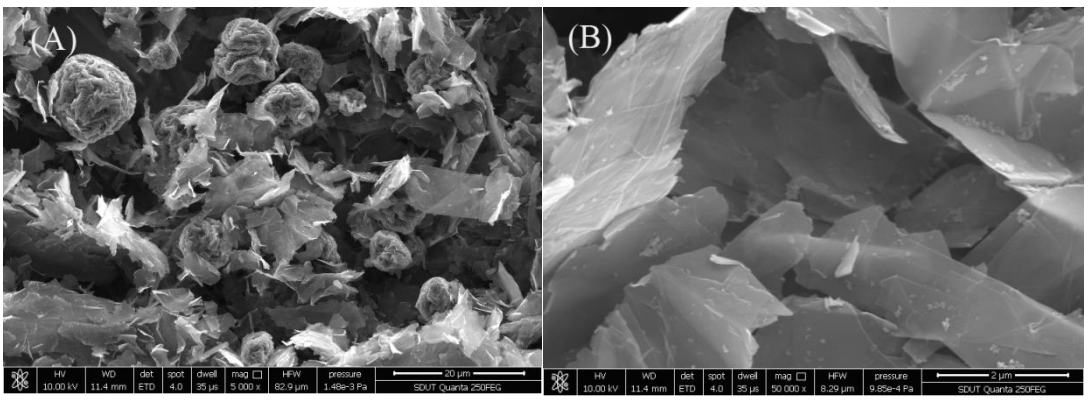

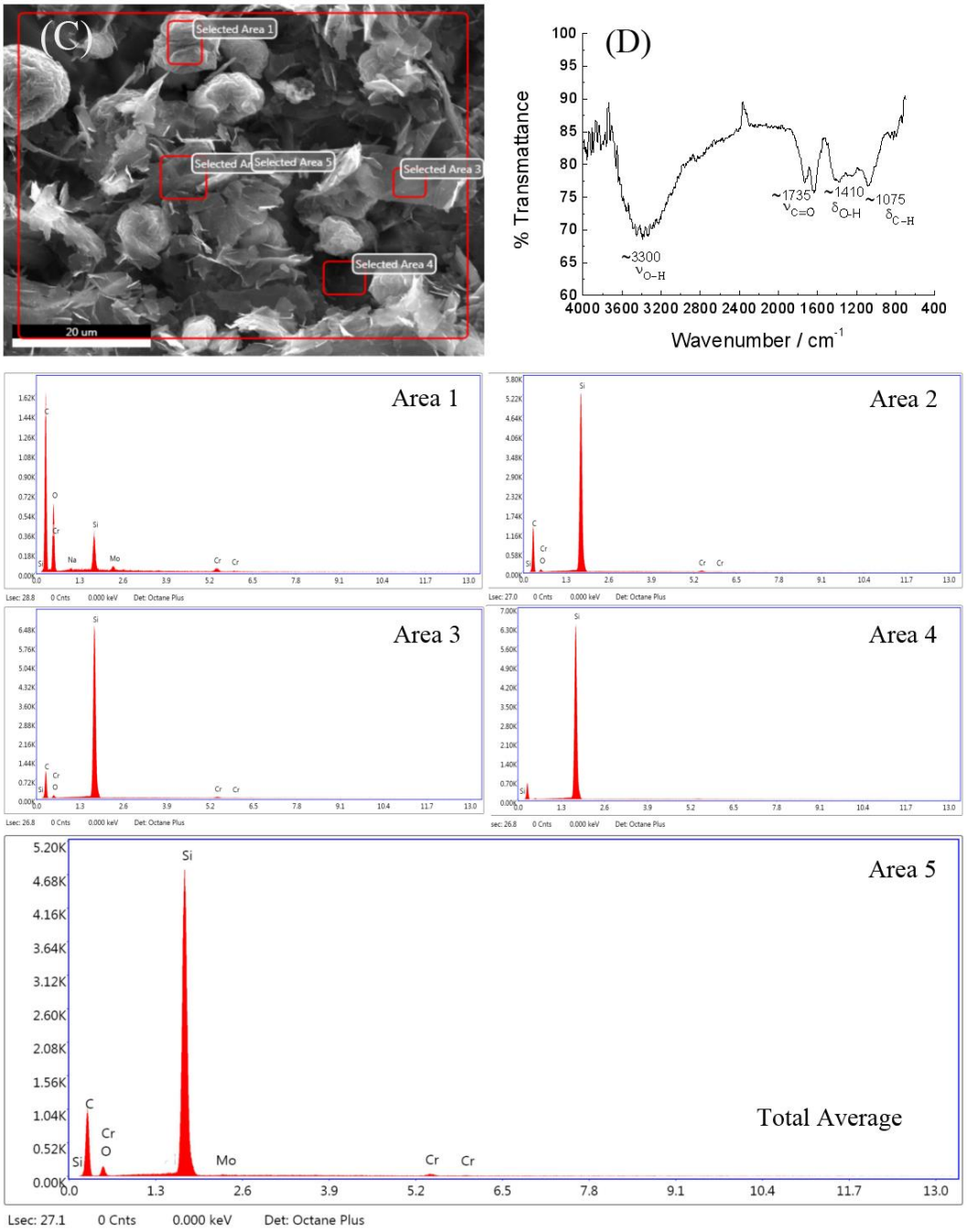

Figure 3. SEM morphology (A), (B) and EDS spectra (C) of the Gr-SiNWs-Si/Pt; (D) FTIR spectrum of the surface of Gr-SiNWs-Si/Pt

3.4 Cyclic voltammetry characters of the Gr-SiNWs-Si/Pt electrode

The photoelectrochemical (PEC) characters of the Gr-SiNWs-Si/Pt electrode in pH 7.0 PBS solution containing 200 μM HQ were studied with cyclic voltammetry measurement on a LK2005 workstation. Fig. 4A shows the comparison of CV curves of HQ electrochemical redox on the Gr-SiNWs-Si/Pt electrode in dark and in light. It can be seen that the electrode permit reduction reaction only without illumination as the solid curve depicts in Fig. 4A, confirming the rectifying property of the

Si/Pt interface in the Gr-SiNWs-Si/Pt electrode. With illumination, both oxidation reaction and reduction reaction are allowed at proper potential. In addition, owing to the photo-induced carriers generated in light, the reduction photocurrents increases to about 3 times of that in dark, demonstrating the PEC property of the Gr-SiNWs-Si/Pt electrode in detection of HQ in solution. Fig. 4B shows the CV curves of HQ reaction on Si/Pt (a), SiNWs-Si/Pt (b) and Gr-SiNWs-Si/Pt (c) electrode, respectively, in 0.1 M pH 7 PBS with illumination. It is clear that the Si/Pt electrode is a poor electrochemical platform for the HQ redox reaction as curve (a) shows in Fig. 4B. However, with the growth of SiNWs, the SiNWs-Si/Pt electrode turns to a usable platform as curve (b) in Fig. 4B depicts. This may be ascribed to the effect of the SiNWs which may act as charge exchange tunnels between the electrode and the solution. Compared to curve (b), the HQ redox peaks on Gr-SiNWs-Si/Pt electrode are much closer and the currents are obviously bigger on curve (c), showing both better electrochemical reversibility and better sensitivity. The results demonstrate that the modifications of SiNWs and graphene are beneficial to the sensing of HQ.

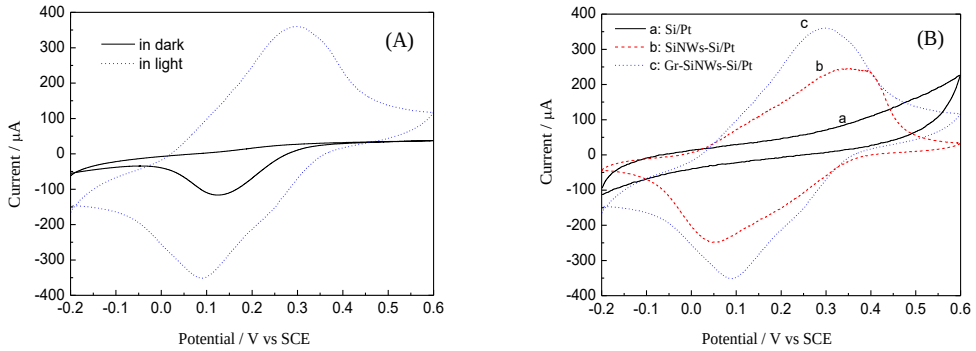

Figure 4. (A) CV character of the Gr-SiNWs-Si/Pt electrode in dark and in light; (B) Comparison of CV curves of Si/Pt (a), SiNWs-Si/Pt (b) and Gr-SiNWs-Si/Pt (c) electrode in light in 0.1 M pH 7 PBS containing 200 μM HQ with a scan rate of 50 mV s^{-1}

3.5 Performance of the Gr-SiNWs-Si/Pt sensor in detection of HQ

To estimate the PEC performance of Gr-SiNWs-Si/Pt electrode in sensing of HQ, a two-electrode system was build with a graphite electrode as the counter electrode at zero bias in pH 7 PBS solution. Photocurrents of the HQ reaction on the work electrode were recorded as the function of the HQ concentration with the illumination of a 5 W white LED light. In comparison, Si/Pt, Gr-Si/Pt and SiNWs-Si/Pt were also tested in the same experiment conditions as the Gr-SiNWs-Si/Pt electrode. Fig. 5A and Fig. 5C depicts the photocurrents of HQ reaction on the Si/Pt and Gr-Si/Pt electrode, respectively, and the plot of the photocurrent as a function of HQ concentration is shown in Fig. 5B and Fig. 5D, respectively. The results illuminate poor stability of photocurrent response to HQ and poor linear relationships on both electrodes. The sensitivity of HQ on Gr-Si/Pt (0.018 μA/μM) is very close to that on Si/Pt (0.016 μA/μM), which indicates the charge exchange ability is limited between the surface of Si/Pt and the modified graphene layer. Fig. 5E and Fig. 5F shows the PEC response of HQ on the SiNWs-Si/Pt electrode and the calibration curve of the photocurrent against the concentration of HQ, respectively. It can be seen that the photocurrent changed immediately after the addition of HQ and

maintains at a steady current within tens of seconds. The response photocurrent increased stepwise for successive injection of 10, 10, 20, 20, 40, 40, 80 and 80 μM HQ, respectively, into pH 7.0 PBS. The calibration curve exhibits a good linear response to HQ in a range from 10 μM to 300 μM with a correlation coefficient of R^2=0.997. The sensitivity to HQ can be obtained from the slope of the plot to be 0.039 μA/μM. It is clear that the growth of SiNWs not only increases the sensitivity of the electrode to HQ, but also enhances the stability of the photocurrent response, which confirms the charge exchange tunnel effect of the SiNWs as mentioned in section 3.4. We tentatively speculate that the SiNWs may act as antennas or lightning rods in tip discharge phenomenon, facilitating the charge exchange between the electrode and the solution. Similar effect can be referred in Ref [24]. Despite the linear photocurrent respond of the HQ on the SiNWs-Si/Pt electrode, the sensitivity is still not satisfactory compare to other works [25-28]. Graphene was supposed to improve the sensitivity of the electrode to HQ. Fig. 5G shows the photocurrent curves of the Gr-SiNWs-Si/Pt electrode in detection of HQ in PEC way at zero bias in pH 7.0 PBS solution. As can be seen, the response photocurrent of HQ increased obviously on the Gr-SiNWs-Si/Pt electrode compared to that on SiNWs-Si/Pt electrode, which is ascribed to the good conductivity and absorption capacity of the graphene. Moreover, the linear relationship (correlation coefficient R^2=0.9996) between the photocurrent and the concentration of HQ was also improved as shown in Fig. 5H. The sensitivity can be obtained from the slop of the linear line to be 0.360 μA/μM which is nearly ten times of that on SiNWs-Si/Pt. The detection limit can be estimated to be 0.3 μM according to the S/N=3 criterion suggested by IUPAC [29]. The analytical performances of the PEC sensor was compared with other works reported in literature for HQ determination and the parameters, including detection technique, sensitivity, linear range and detection limit (LOD), are listed in Table 1.

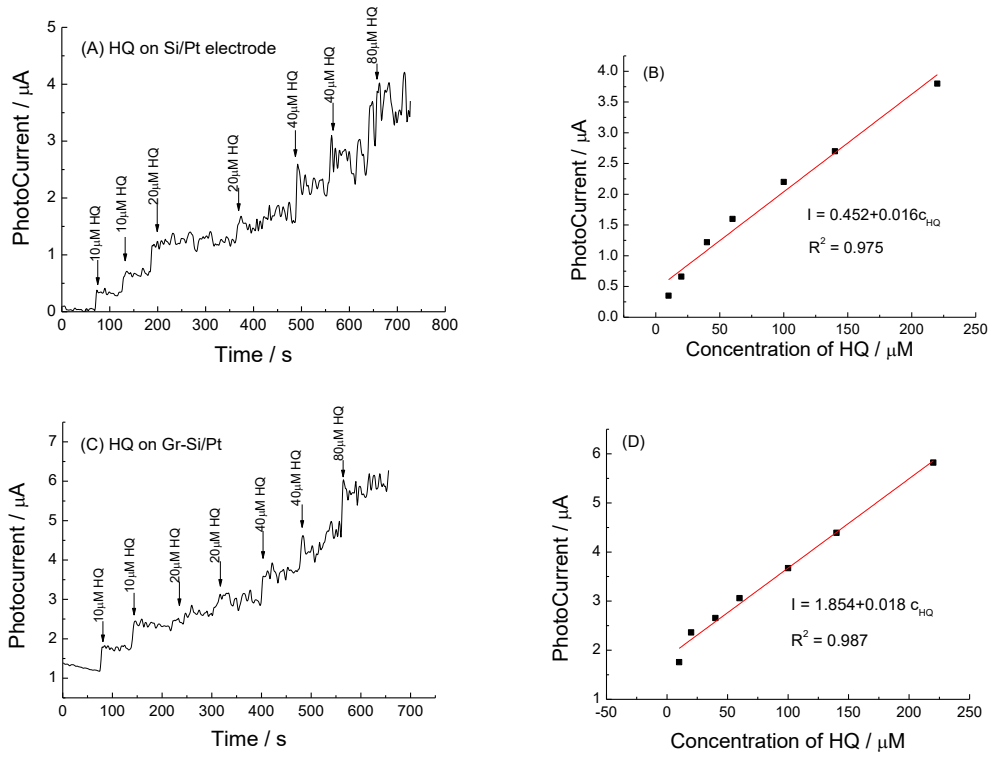

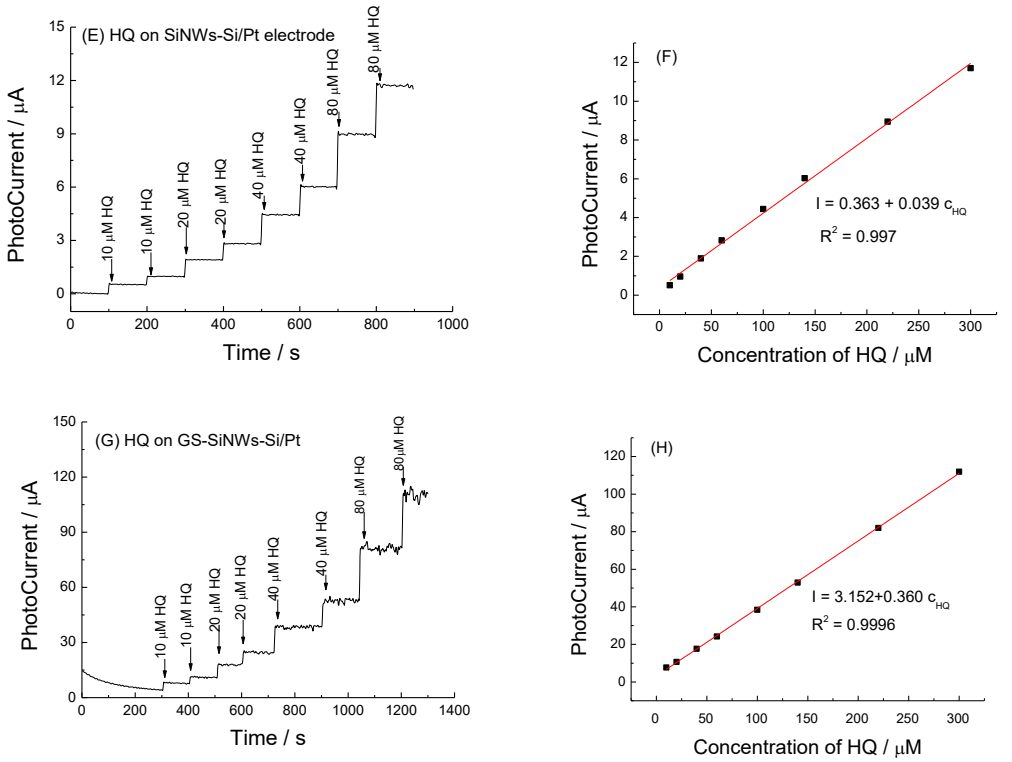

Figure 5. Photocurrent curves and the linear fitting between photocurrent and HQ concentration on Si/Pt (A, B), Gr-Si/Pt sensor (C, D), SiNWs-Si/Pt (E, F) and Gr-SiNWs-Si/Pt (G, H) in a two-electrode system with a graphite plate as counter electrode to successive addition of 10 μM, 10 μM, 20 μM, 20 μM, 40 μM, 40 μM, 80 μM and 80 μM HQ, respectively, into PBS at zero bias under 5 W white light LED illumination.

Table 1. Comparison of the sensitivity, linear range and LOD of different methods for HQ detection

Modified electrode	Detection technique	Sensitivity (μA/μM)	Linear range (μM)	LOD (μM)	Ref.
CNNS-CNT	DPV	0.0386	0.31–13.1	0.13	[25]
Pal/NGE	DPV	0.49	1–50	0.8	[26]
PGCE	CV	0.136	10–300	3.57	[27]
MWCNTs/CTS/Au/GCE	DPV	0.046	0.5–1500	0.17	[28]
Graphene-Pd/GCE	DPV	1.098	75–5000	1.25	[30]
Au-PdNF/rGO GCE	DPV	0.147	1.6-100	0.5	[31]
AuNPs/Fe_3O_4-APTES-GO GCE	Amperometry	0.0018	3 – 137	1.1	[32]
AuNPs-MPS CPE	SWVA	0.0731	10–1000	1.2	[33]
Gr-SiNWs-Si/Pt	Photocurrent at zero bias	0.36	10–300	0.3	This work

The data listed in Table 1 verifies a good sensitivity, a wide linear range and a low LOD of the Gr-SiNWs-Si/Pt PEC sensor. It is worth noting that the PEC sensor suggested in this work is independent

of power supply and works at zero bias voltage in a simple two-electrode system, which facilitates the miniaturization and portable demands to sensors. In fact, this sensor has been tested with a digital multimeter (FK830L, FUKE) under natural sunlight (14:00-14:30, p.m. in fifth August, a sunny day in Zibo, northern latitude 36°48" and east longitude 117°59") in PEC sensing of HQ. The photocurrent response to successive addition of 20 μM HQ was stable at about 7 μA to each addition and the statistic data is provided in Table 2, demonstrating its reliability as a portable sensor.

Table 2. Statistical data in HQ detection by the Gr-SiNWs-Si/Pt sensor

HQ added (μM)	20	20	20	20	20	20	20	Standard deviation	RSD (%)
Each photocurrent response (μA)	7.03	6.95	6.99	7.11	7.21	6.91	6.99	0.102	1.46
HQ detected (μM)	19.53	19.31	19.42	19.75	20.03	19.19	19.42	0.285	1.46
Recovery (%)	97.65	96.55	97.1	98.75	100.2	95.95	97.1	1.438	1.46

3.6 Mechanism of the PEC sensor in sensing of HQ

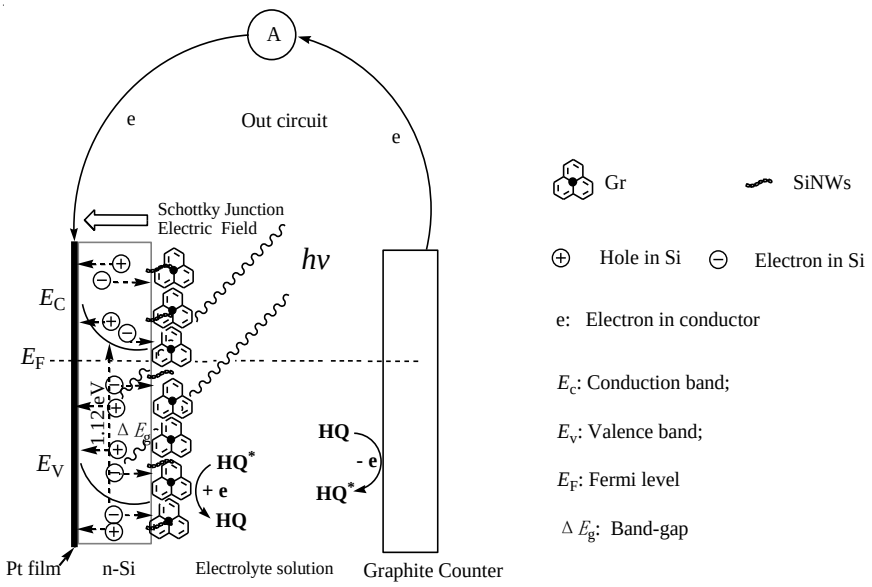

Figure 6. Proposed mechanism for photoelectrochemical sensing of HQ

Fig. 6 depicts a schematic representation of the PEC sensor for the detection of HQ. With illumination, large quantity of electron-hole pairs generated in the illuminated areas in Si wafer and then were separated by the static electric field of the Schottky junction at the Si/Pt interface. The electrons were collected to the Si side before transmitted to the graphene layer though the tunnel effect of the SiNWs on the Si wafer. The holes were collected at the Pt side according to the direction of static electric field. As schemed in Fig. 6, HQ was oxidized to be HQ^* on the graphite counter electrode and the lost

electrons were transmitted through the out circuit to the Pt side and recombined with the holes collected from the illuminated Si wafer. Meanwhile, HQ^*, the oxidized HQ, reduced on the graphene layer on the Gr-SiNWs-Si/Pt electrode by capturing the electrons transmitted from the Si wafer through the SiNWs tunnels. Thus, a loop circuit was formed. The photocurrent is in linear relationship to the concentration of HQ and can be detected by the galvanometer in the circuit.

3.7 The anti-interference performance of the PEC sensor in detection of HQ

The anti-interference performance of the Gr-SiNWs-Si/Pt electrode was evaluated against common pollutants which may interfere HQ detection, especially the isomer, catechol (CC). Considering Cu^{2+} and Pd^{2+} are the most common heavy metal in industrial wastewater and *L*-cysteine, glutamic acid and uric acid are the usual protein wastes in domestic wastewater, they were used as interferents in the anti-interference experiment besides CC. Fig. 7 shows the photocurrent response of the Gr-SiNWs-Si/Pt sensor to the above mentioned polutants that may exist in environment water. Results show that most substances have no interference to the sensor in the HQ detection except very slight interference from CC, demonstrating a good selectivity to HQ of the proposed sensor.

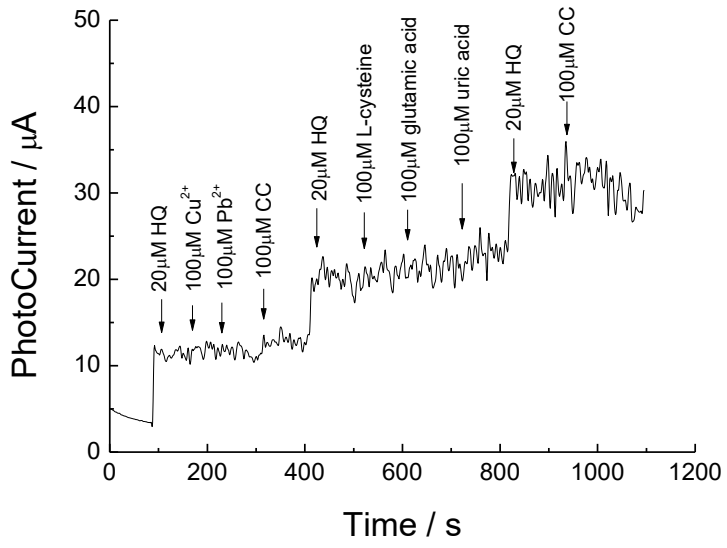

Figure 7. Photocurrent response of Gr-SiNWs-Si/Pt to successive addition of 20 μM HQ, 100 μM Cu^{2+}, 100 μM Pb^{2+}, 100 μM CC, 20 μM HQ, 100 μM *L*-cysteine, 100 μM glutamic acid, 100 μM uric acid, 20 μM HQ and 100 μM CC in PBS

3.8 Stability and reproducibility of the sensor

The measurement stability of the Gr-SiNWs-Si/Pt sensor was evaluated by performing intermittent detection (5 times on every other day) of 20 μM HQ in 3 weeks. As Fig. 8A illuminated, the photocurrent response retains 93% of its original value after 20 days of intermittent usage and storage in the PBS. To investigate the reproducibility of the sensor, seven Gr-SiNWs-Si/Pt electrodes were

prepared under the same conditions and the photocurrent responses to HQ were performed 5 times on each electrode. Fig. 8B shows the detection results of 20 μM HQ in PBS on the seven electrodes. It can be seen that the relative standard deviation (RSD) is lower than 7% between the seven electrodes, demonstrating a good reproducibility of the PEC sensor.

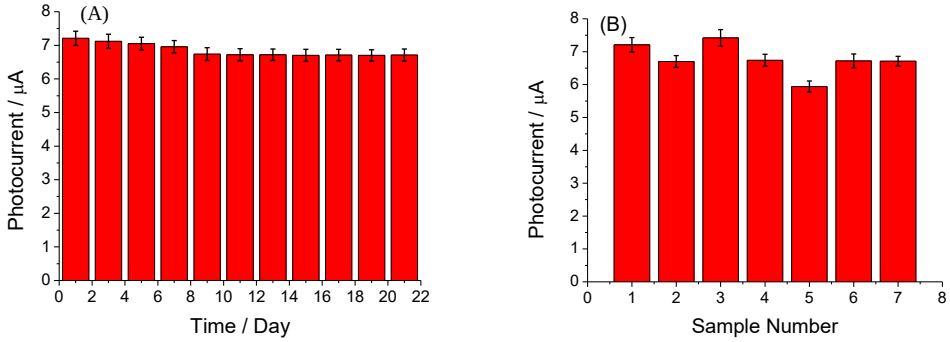

Figure 8. Stability (A) and reproducibility (B) of the Gr-SiNWs-Si/Pt sensor in PEC detection of 20 μM HQ (Error bars are the standard deviation for five consecutive measurements)

4. CONCLUSIONS

A novel photoelectrochemical sensor for sensing of HQ based on Gr-SiNWs-Si/Pt electrode was proposed in the present work. The Schottky junction of Si/Pt in the sensor was proved to be efficient in the separation of light-induced electron-hole pairs. The SiNWs on the surface of Si wafer enhance the efficiency of the photoelectric transmission and play key role in the charge exchange between the Si wafer and graphene layer in detection of HQ in solution. The modified graphene layer enhances the sensitivity of the PEC sensor about ten times compared to SiNWs-Si/Pt. The sensor shows good sensitivity, wide linear range and a low detection limit in HQ detection. Furthermore, this proposed sensor works in a two-electrode system at a zero bias voltage and provides a portable and simple device for rapid PEC determination.

ACKNOWLEDGEMENTS
This work was supported by Research Foundation of PhD at Shandong University of Technology (No: 4041/418039) and University Student Innovation Training Project of China (No: 4051/117207).

References

1. Z. Hong, L. Zhou, J. Li and J. Tang, *Electrochim. Acta*, 109 (2013) 671.
2. M. Buleandra, A.A. Rabinca, C. Mihailciuc, A. Balan, C. Nichita, I. Stamatin and A.A. Ciucu, *Sens. Actuators B*, 203 (2014) 824.
3. J. Zhou, X. Li, L. Yang, S. Yan, M. Wang, D. Cheng, Q. Chen, Y. Dong, P. Liu, W. Cai and C. Zhang, *Anal. Chim. Acta*, 899 (2015) 57.
4. G. Marrubini, E. Calleri, T. Coccini, A.F. Castoldi and L. Manzo, *Chromatographia*, 62 (2005) 25.
5. J. Wittig, S. Wittemer and M. Veit, *J. Chromatogr. B*, 761 (2001) 125.
6. S. Moldoveanu and M. Kiser *J. Chromatogr. A*, 1141 (2007) 90.

7. Sirajuddin, M.I. Bhanger, A. Niaz, A. Shah and A. Rauf, *Talanta*, 72 (2007) 546.
8. L.A. Goulart and L.H. Mascaro, *Electrochim. Acta*, 196 (2016) 48.
9. M.U.A. Prathap, B. Satpati and R. Srivastava, *Sens. Actuators B*, 186 (2013) 67.
10. H.S. Han, J.M. You, H. Seol, H. Jeong and S. Jeon, *Sens. Actuators B*, 194 (2014) 460.
11. S. Erogul, S.Z. Bas, M. Ozmen and S. Yildiz, *Electrochim. Acta,* 186 (2015) 302.
12. W. Cheng, J. Pan, J. Yang, Z. Zheng, F. Lu, Y. Chen and W. Gao, *Microchim. Acta,* 185 (2018) 263.
13. J. Gayathri, K.S. Selvan and S.S. Narayanan, *J. Solid State Electrochem.,* 22 (2018) 2879.
14. S.S. Patil, N.L. Tarwal, H.M. Yadav, S.D. Korade, T.S. Bhat, A.M. Teli, M.M. Karanjkar, J.H. Kim and P.S. Patil, *J. Solid State Electrochem.*, 22 (2018) 3015.
15. R.S. Moakhar, G.K.L. Goh, A. Dolati and M. Ghorbani, *Appl. Catal. B*, 201 (2017)411.
16. D. Chen, D. Jiang, X. Du, L. Zhou, L. Huang, J. Qian, Q. Liu, N. Hao, Y. Li and K. Wang, *Electrochim. Acta*, 215 (2016) 305.
17. Z. Yue, W. Zhang, C. Wang, G. Liu and W. Niu, *Mater. Lett.* 74 (2012) 180.
18. H. Li, Y. Ban, Q. Gao and H. Wu, *Sci. Adv. Mater.*, 4 (2012) 1.
19. H. Li, Q. Gao, L. Chen and W. Hao, *Sens. Actuators B*, 173 (2012) 540.
20. H. Li, W. Hao, J. Hu and H. Wu, *Biosens. Bioelectron.*, 47 (2013) 225.
21. H. Wu, J. Hu, H. Li and H. Li, *Sens. Actuators B*, 182 (2013) 802.
22. H. Zhang, Q. Gao and H. Li, *J. Solid State Electrochem.*, 20 (2016) 1565.
23. D.J. Kim, G.S. Kim, N.W. Park, W.Y. Lee, Y. Sim, K.S. Kim, M.J. Seong, J.H. Koh, C.H. Hong and S.K. Lee, *J. Alloys Comp.*, 612 (2014) 265.
24. L. He, X. Zhang, W. Wang and H Wei, *Appl. Surf. Sci.*, 382 (2016) 323.
25. H. Zhang, Y. Huang, S. Hu, Q. Huang, C. Wei, W. Zhang, W. Yang, P. Dong and A. Hao, *Electrochim. Acta*, 176 (2015) 28.
26. Y. Wu, W. Lei, M. Xia, F. Wang, C. Li, C. Zhang, Q. Hao and Y. Zhang, *Appl. Clay Sci.*, 162 (2018) 38.
27. H. Zhang, S. Li, F. Zhang, M. Wang, X. Lin, H. Li, *J. Solid State Electrochem.*, 21 (2017) 735.
28. Y. Shen, D. Rao, Q. Sheng and J. Zheng, *Microchim. Acta*, 184 (2017) 3591.
29. A.M. Committee, *Analyst*, 112 (1987) 199.
30. M. Zhang, F. Gan and F. Cheng, *Res. Chem. Intermed.*, 42 (2016) 813.
31. Y. Chen, X. Liu, S. Zhang, L. Yang, M. Liu, Y. Zhang and S. Yao, *Electrochim. Acta*, 231 (2017) 677.
32. S. Erogul, S.Z. Bas, M. Ozmen and S. Yildiz, *Electrochim. Acta*, 186 (2015) 302.
33. J. Tashkhourian, M. Daneshia, F. Nami-Anaa, M. Behbahani and A. Bagheri, *J. Hazard Mater.*, 318 (2016) 117.